Supporting Information

Manganese Oxide/iron Carbide Encapsulated in Nitrogen and Boron Co-doped Carbon Nanowire Networks as The Accelerated Alkaline Hydrogen Evolution and Oxygen Reduction Bi-functional Electrocatalysts

Zhuo Liu,[a] Fei Guo, [a] Lina Han, [b] Jie Xiao, [a] Xiaoyuan Zeng, [a] Chengxu Zhang, [a] Peng Dong, [a] Mian Li,* [a] Yingjie Zhang,* [a,b]

[a] *National and Local Joint Engineering Laboratory for Lithium-ion Batteries and Materials Preparation Technology, Key Laboratory of Advanced Battery Materials of Yunnan Province, Faculty of Metallurgical and Energy Engineering, Kunming University of Science and Technology, Kunming 650093, PR China*

[b] *Faculty of Material Science and Engineering, Kunming University of Science and Technology, Kunming 650093, China*

* Corresponding author.

E-mail addresses: mianzi2009@126.com, lim148@kmust.edu.cn (M. Li); zyjkmust@126.com (Y. Zhang)

1. Experimental Section

1.1. The detailed conditions for electrospinning.

For the electrospinning, all as-obtained precursor slurries were loaded into the plastic syringes with the inner diameter of pinhead is 0.80 mm. the voltage applied for electrospinning was 23 kV and the flow rates of precursor slurries are controlled as 1 mL h^{-1} by using the pump. The stainless steel mesh was used to collect the precursor networks. The distance between the orifices and the stainless steel mesh electrodes were all controlled as ~15 cm. The as-electrospun precursor networks were then calcinated at different temperatures for 2 h in nitrogen atmosphere.

1.2. Synthesis of the precursor networks for Fe@BNPCFs-900 and Mn@BNPCFs-900 samples.

For comparison, the Fe@BNPCFs-900 and Mn@BNPCFs-900 samples have been prepared as well. 3.3 g of PVP powder and 1.0 g of HA were first dissolved into 40.0 mL DMF to produce the HA-PVP-DMF solution. Then, 1.40 g $Fe(AC)_2 \cdot 4H_2O$ or 1.52 g $Mn(AC)_2 \cdot 2H_2O$ were severally added into the as-prepared HA-PVP-DMF solutions. The obtained mixtures were further stirred for another 12 h to acquire the homogeneous precursor slurries [i.e., $Fe(AC)_2$-HA-PVP-DMF and $Mn(AC)_2$-HA-PVP-DMF]. Following closely, the electrospinning technique was utilized for weaving the $Fe(AC)_2$-HA-PVP-DMF and $Mn(AC)_2$-HA-PVP-DMF precursor slurries into the $Fe(AC)_2$/HA/PVP and $Mn(AC)_2$/HA/PVP precursor networks.

1.3. Physical characterization of precursor networks, FeMn@BNPCFs-T (T= 600, 700, 800, 900 and 1000 ℃), Fe@BNPCFs-900 and Mn@BNPCFs-900 control samples.

The scanning electron microscopy (SEM) was performed using a Philips XL-30 ESEM equipped with an energy-dispersive X-ray spectroscopy (EDS) analyzer. The transmission electron microscopy (TEM), high-angle annular dark field scanning transmission electron microscopy (HAADF) and scanning transmission electron microscopy (STEM) were performed on a high-resolution Hitachi JEM-2100 system equipped with an EDX analyzer. The wide-angle X-ray diffraction (XRD) patterns were obtained on an X-ray D/max-2200 vpc (Rigaku Corporation, Japan) instrument operated at 40 kV and 20 mA using Cu Kα radiation (*k* 0.15406 nm). The N_2 adsorption-desorption isotherms were performed on an ASAP 2020 (Micromeritics, USA). Before the measurements, the samples were degassed in vacuum at 120 °C for 5 h. The Brunauer-Emmett-Teller (BET) method was utilized to calculate the BET specific surface area using adsorption data. The pore size distribution was derived from the adsorption branch by using the Barrett-Joyner-Halenda (BJH) model. The Raman spectroscopy patterns were obtained using a confocal microprobe Raman system (HR 800, JobinYvon). The surface analyses of catalysts were carried out by X-ray photoelectron spectroscopy (XPS) on an ESCA LAB spectrometer (USA) using a monochromatic Al Kα source (*hv* 1486.6 eV). The binding energies were calibrated by using the containment carbon (C1s 284.6 eV). The Fe and Mn contents along catalyst's surfaces were determined by inductively coupled plasma optical emission spectrometry (ICP-OES) with a PerkinElmer Optima 3300 DV spectrometer.

1.4. ***Electrochemical characterization of various FeMn@BNPCFs-T (T= 600, 700, 800, 900 and 1000 ℃), Fe@BNPCFs-900 and Mn@BNPCFs-900 control samples toward HER and ORR in alkaline condition.***

Electrochemical measurements were performed at room temperature by using a rotating disk electrode (RDE; 5 mm in diameter with a geometric area of 0.19625 cm^2) or rotating ring-disk electrode (RRDE; 5.5 mm in diameter with a geometric area of 0.23758 cm^2) as the working electrode both in 0.1 M KOH (for ORR) and 1.0 M KOH (for HER). Pt wire was used as counter electrode (for HER test, the counter electrode was carbon rod) and Ag/AgCl was used as reference electrodes. All potentials appeared in this paper are referred to reversible hydrogen electrode, the potentials recorded (referred to Ag/AgCl) in each experiment were calculated using the formula $E_{RHE} = E_{Ag/AgCl} + 0.059\ pH + 0.197\ V$, where E_{RHE} is a potential *vs.* reversible hydrogen electrode (RHE), $E_{Ag/AgCl}$ is a potential *vs.* Ag/AgCl electrode, and pH is the pH value of electrolyte. All current densities are the ratios of recorded currents to the geometric area of electrode.

In order to prepare the working electrodes, 3 mg of as-synthesized catalyst powders were dispersed in 1 mL Nafion solution (0.5 wt%) with 60 min of ultrasonication to generate the homogeneous inks. Following closely, 30 uL of the dispersed slurry was transferred onto the RDE or RRDE with the catalyst loading amount of 0.306 mg cm^{-2}. Finally, the as-prepared catalyst film was dried at room temperature.

In the electrochemical testing processes for HER and ORR, the Tafel polarization curves were plotted as potentials (*E vs. RHE*) *vs.* log |*j*(mA cm^{-2})| to get the Tafel plots for assessing the HER and ORR kinetics of the resultant catalysts. By

fitting the linear portion of the Tafel plots to the Tafel equation ($\eta = b \log (j) + a$), the Tafel slopes (b values) can be obtained. All data were reported without iR compensation.

The roughness (R) and electrochemical specific active area (ECSA) were calculated by using **Equations S1** and **S2**:

$$R = C_{sample}/C_{GCE} \quad \textbf{(S1)}$$

$$ECSA = R \times A_{GCE} \quad \textbf{(S2)}$$

Where $A = 0.19625$ cm^2 in this work.

The turnover frequency (TOF) values of the optimal catalyst were calculated from the equation **S3**:

$$TOF = j \times A/(4\times F \times m) \quad \textbf{(S3)}$$

Where the j value is current density obtained at each potential, A is the area of the electrode, F is the Faraday constant (96 485 C mol^{-1}), and m is the molar number of active material loaded on the electrode.

In addition, for the ORR test, in order to further verify the ORR catalytic pathways of various catalysts, we also conducted the RRDE measurements at the potential scan rate of 5 mV s^{-1} with an electrode rotation speed of 1600 rpm. Meanwhile, the operating potential of Pt ring was set at 0.5 V *vs.* Ag/AgCl in 0.1 M KOH for RRDE tests. The electron transfer numbers **(n)** were also calculated from the **Equation S4** and the H_2O_2 formation yields were calculated from the **Equation S5** based on the RRDE data:

$$n = \frac{4I_D}{(I_D + I_R / N)} \quad \textbf{(S4)}$$

$$\% \ HO_2^- = \frac{200 I_R)}{(I_D N + I_R)} \quad \textbf{(S5)}$$

Where N is the collection efficiency with a value of 0.37, I_D and I_R are the faradic-disk and -ring currents respectively.

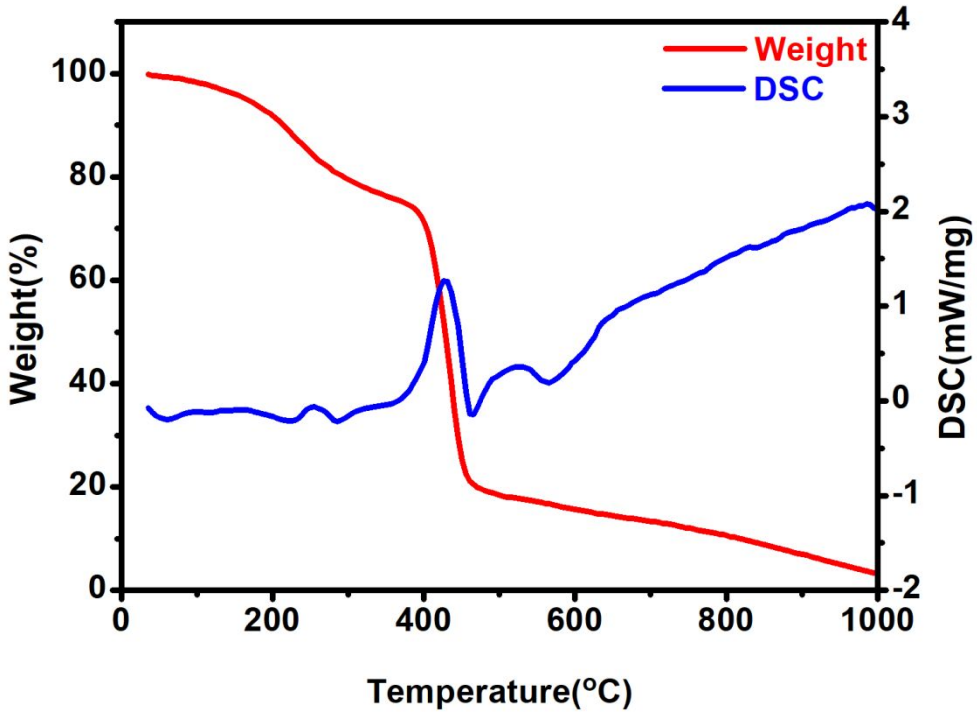

Figure S1. The DSC-TGA curves of the precursor networks, in the flowing of pure nitrogen with a temperature rating of 10 ℃ min^{-1}.

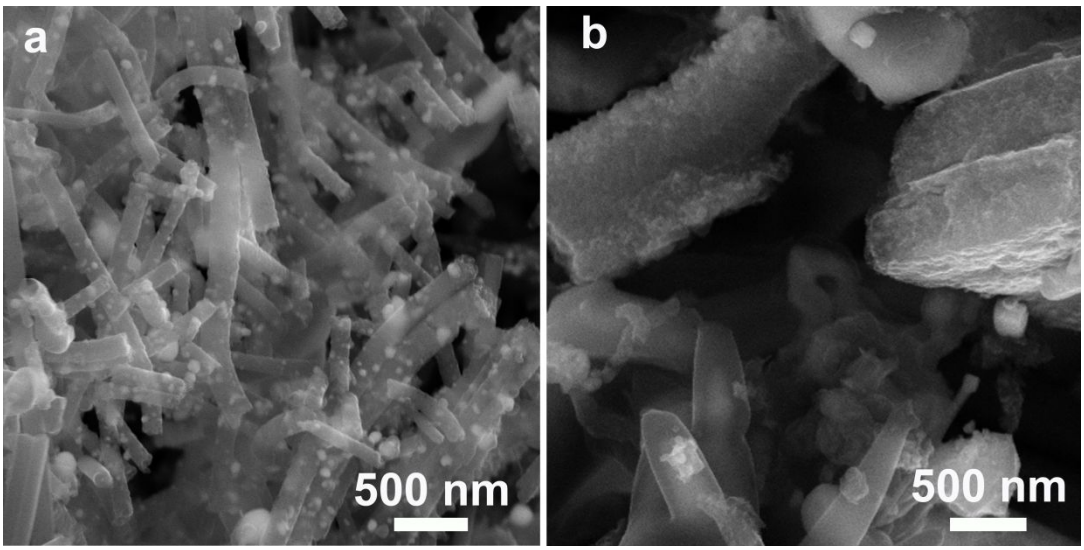

Figure S2. The SEM images of the Fe@BNPCFs-900 **(a)** and Mn@BNPCFs-900 **(b)**

control sample.

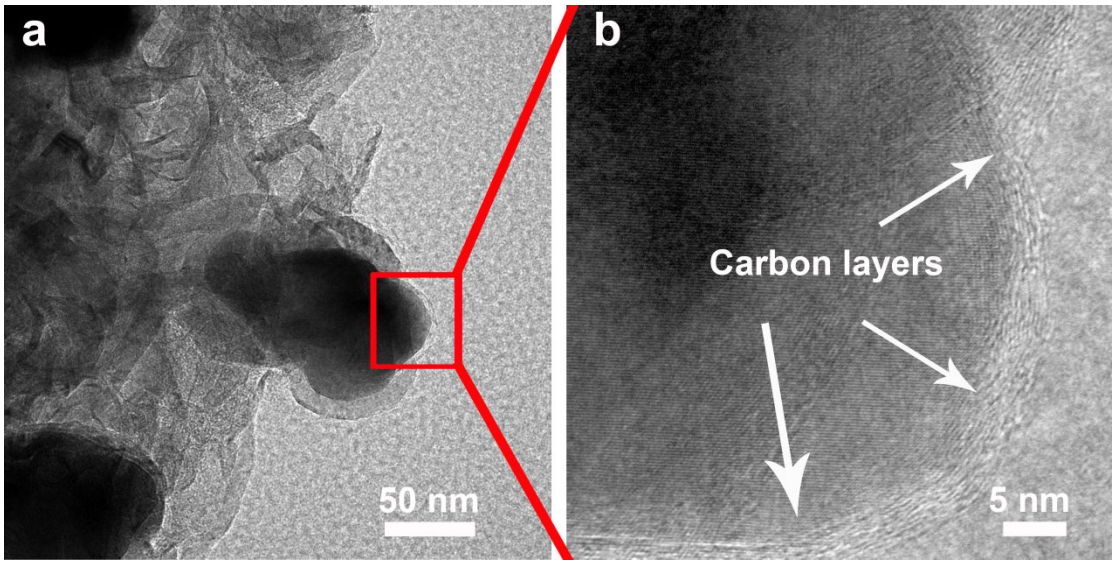

Figure S3. The TEM **(a)** and HRTEM **(b)** images of the FeMn@BNPCFs-900 control sample; **b** is the amplification of red square area showed in **a.**

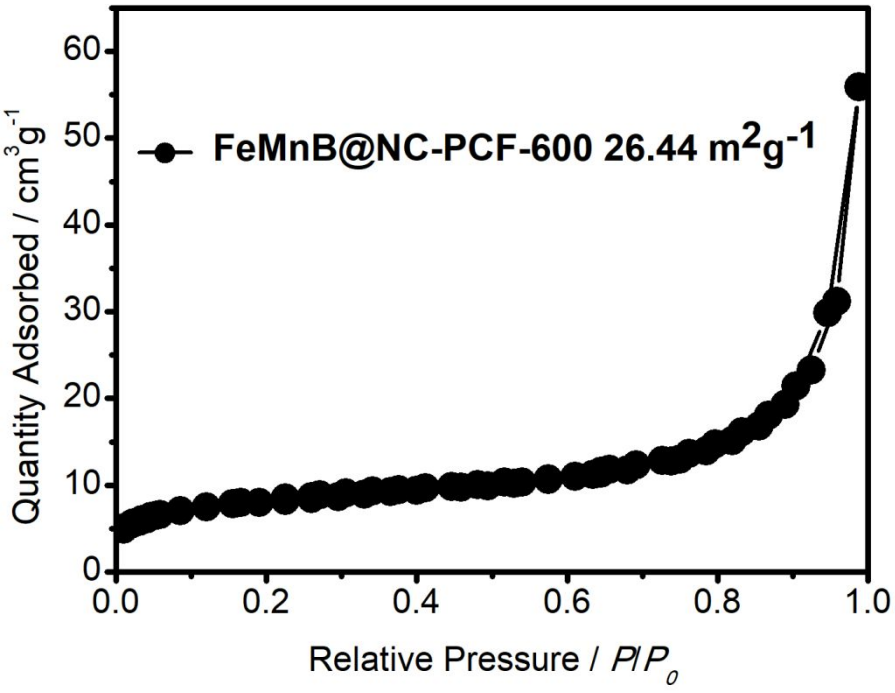

Figure S4. The nitrogen adsorption–desorption isotherm of the FeMn@BNPCFs-600 control sample.

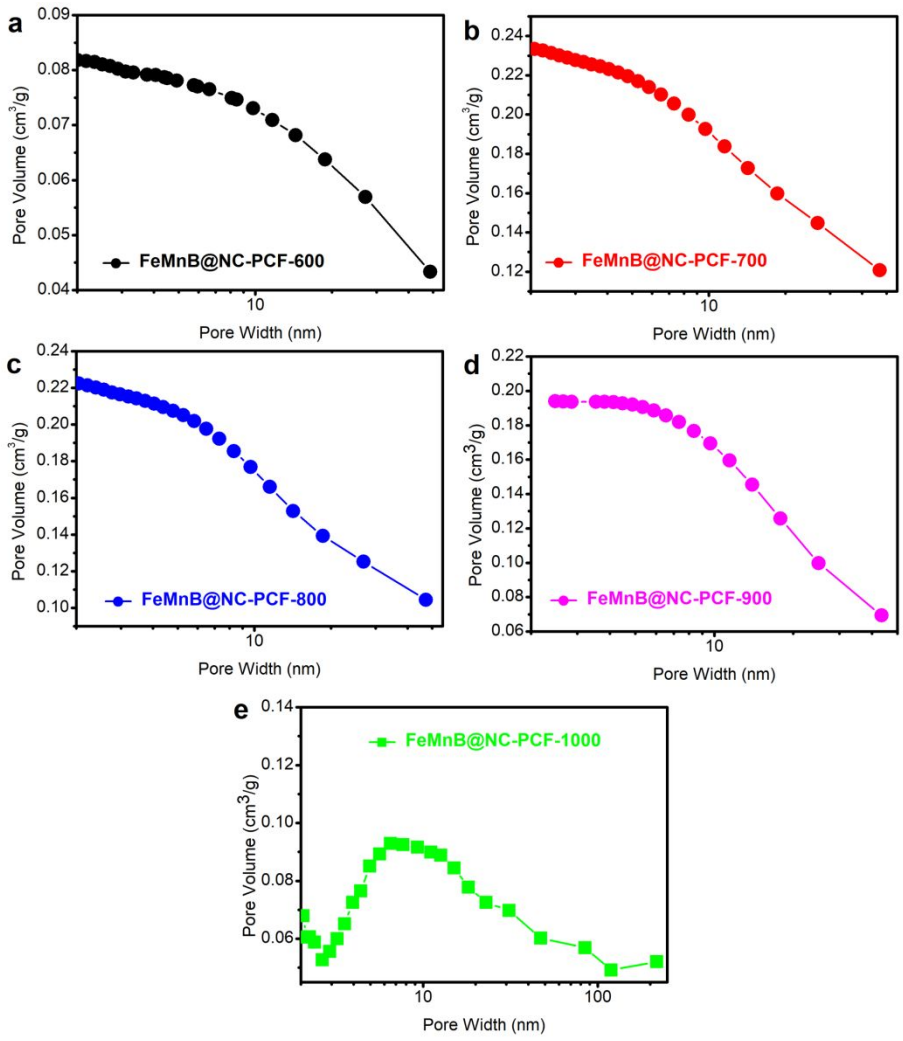

Figure S5. The pore size distribution plots of **(a)** FeMn@BNPCFs-600, **(b)** FeMn@BNPCFs-700, **(c)** FeMn@BNPCFs-800, **(d)** FeMn@BNPCFs-900 and **(e)** FeMn@BNPCFs-1000 control samples.

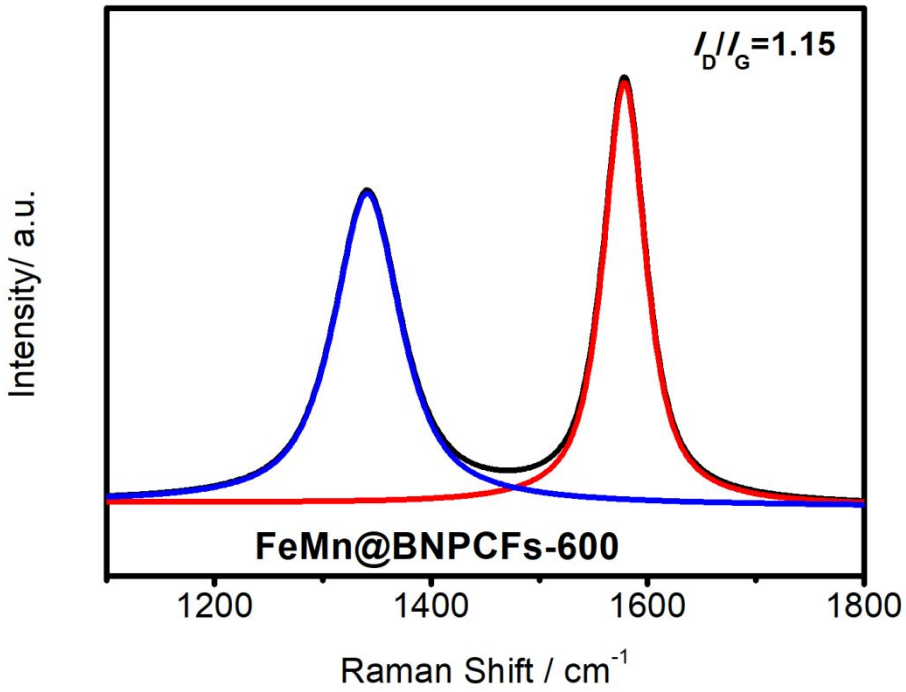

Figure S6. The Raman spectrum of resultant FeMn@BNPCFs-600 material.

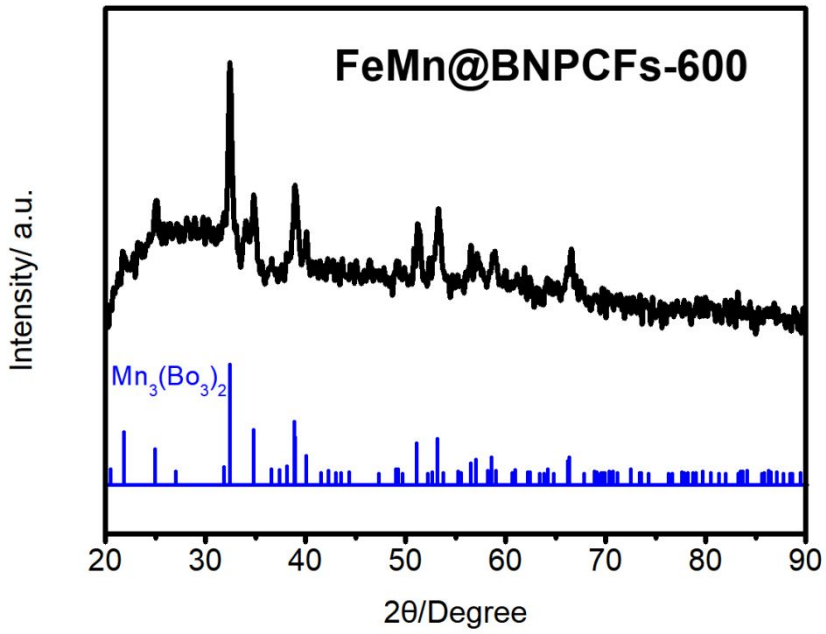

Figure S7. The XRD pattern of the resultant FeMn@BNPCFs-600 sample.

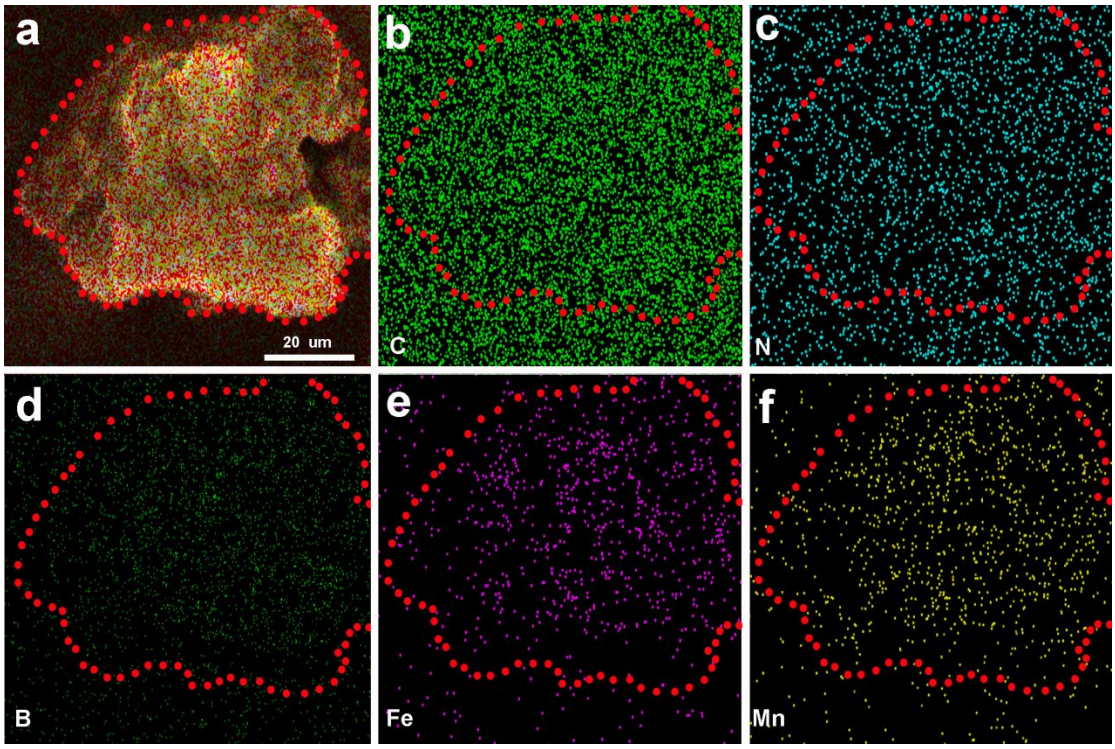

Figure S8. The SEM-EDX mapping of the resultant FeMn@BNPCFs-900 sample: **(a)** overlapped signals of each element and the distribution states of **(b)** C, **(c)** N, **(d)** B, **(e)** Fe and **(f)** Mn elements.

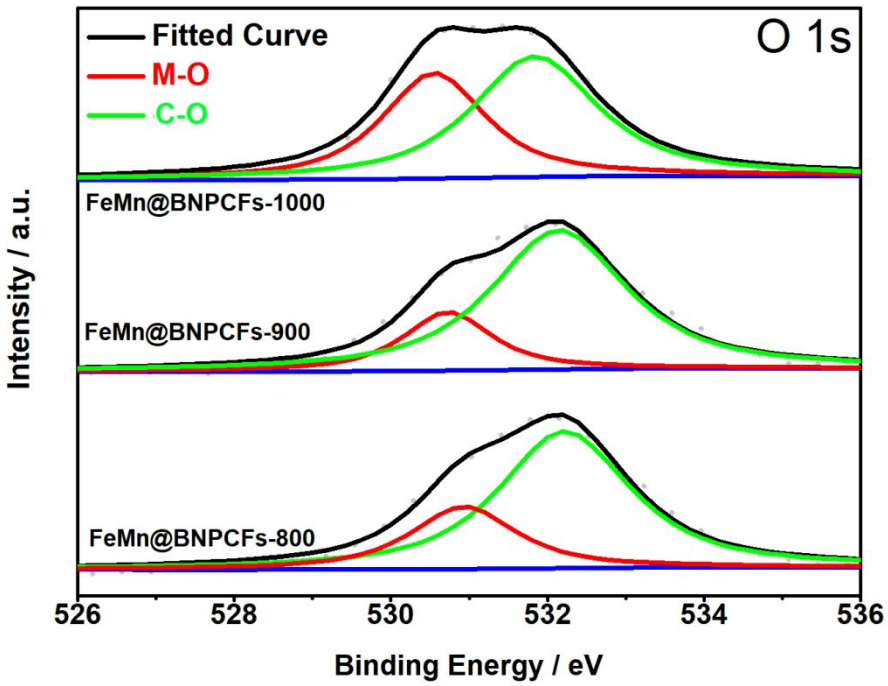

Figure S9. The high-resolution O 1s spectra of resultant FeMn@BNPCFs-800, FeMn@BNPCFs-900 and FeMn@BNPCFs-1000 materials.

Table S1 A comparison on HER catalytic data between our catalysts and other reported non-precious metal based HER catalysts.

Catalysts	η_{10} (mv)	η_{onset} (mv)	Tafel Slope (mV dec^{-1})	Catalyst Loading (g cm^{-2})	Medium	References
FeMn@BNPCFs-600	431	203	226.94	0.306	1 M KOH	This work
FeMn@BNPCFs-700	383	155	212.81	0.306	1 M KOH	
FeMn@BNPCFs-800	311	97	127.69	0.306	1 M KOH	
FeMn@BNPCFs-900	247	49	104.89	0.306	1 M KOH	
FeMn@BNPCFs-1000	325	126	130.51	0.306	1 M KOH	
Fe-promoted MoP	195	150	49	0.071	0.5 MH_2SO_4	*Appl. Catal. A-Gen.* **2016**, *524*, 134-138
0.05Mn-MoP	199	210	49	0.46	0.5 MH_2SO_4	*App. Surf. Sci.* **2021**, *551*, 149321
MnFeO-NF-0.8	186	172	74	0.46	1 M KOH	*Nanoscale*, **2020**, *12*, 19992
NiFeMn-LTH/FM-NS /NF-4	110	191	80	0.46	1 M KOH	*Nanoscale*, **2019**, *11*, 20797
Mn-FeP	175	153	103.6	-	0.5 MH_2SO_4	*App. Surf. Sci.* **2020**, *510*, 145427
NiFe LDH/NF	210	190	58.9	-	1 M KOH	*Science* **2014**, *345*, 1593
Fe^{13+}-WS_2/CC	160	176	77.3	-	0.5 M HCl	*FlatChem* **2021**, *27*, 100247
Fe_2P	300	201	126	-	1 M KOH	*ACS. Appl. Mater. Interfaces* **2016**, *8*, 12798−12803
Ni-Fe-Mn	68	-	64	0.46	1 M KOH	*Int. J, Hydrogen Energ.* **2020**, *45*, 24670-24683
Fe-Ni@NCF	219	207	79.1	-	1 M KOH	*Int. J, Hydrogen Energ.* **2020**, *45*, 12237-12243.
FeP/NF	157	-	97	1	1 M KOH	*Chem. Sci.* **2018**, *9*, 8590-8597.
Mesoporous Mn-FeP	173	-	95	0.51	1 M KOH	*ACS Sustainable Chem. Eng.* **2019**, *7*, 12419–12427
FeP/NCNSs	205		70	0.6	1 M KOH	*ACS Sustainable Chem. Eng.* **2018**, *6*, 11587-11594.
P-$FeMnO_x$	97	150	126.8	-	1 M KOH	*ACS Sustainable Chem. Eng.* **2021**, *9*, 5963–5971
Cu@$Mn(OH)_2$	248	182	184	-	1 M KOH	*Nano Research* **2018**, *11*, 1798–1809
Fe-H_2cat	-	343	77	-	1 M KOH	*Chem* **2018**, *4*, 1139-1152
Fe/P/C0.5-800	256	110	53.6	0.46	1 M KOH	*Nano Energy* **2017**, *33*, 221-228
Fe@C-SN/50	550	358	123	0.55	1 M KOH	*Energy Fuels.* **2021**, *35*, 16046−16053
Fe@N-C/RGO	400	248	100	-	1 M KOH	*Faraday Discuss.* **2014**, *176*, 135-151
Porous FeP nanosheets	253	100	67	-	1 M KOH	*Chem. Commun.* **2013**, *49*, 6656

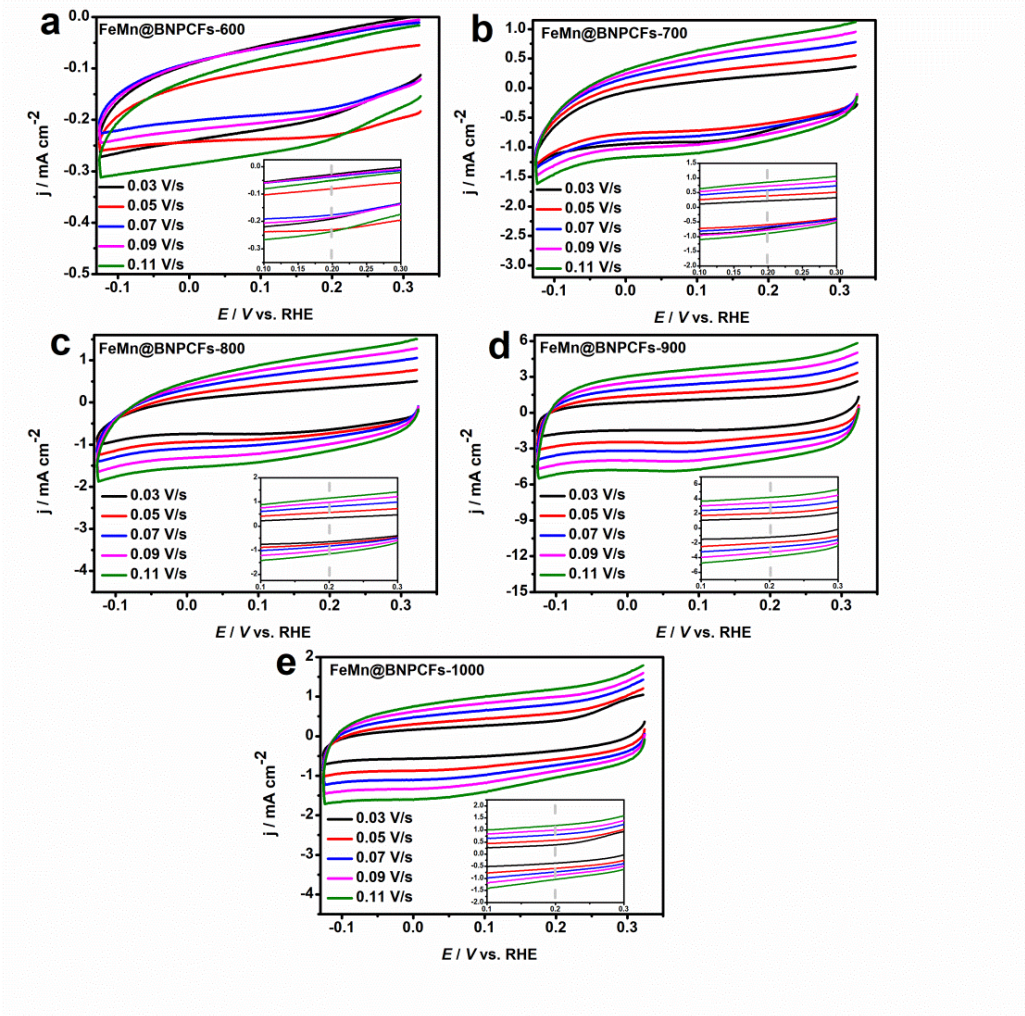

Figure S10. CV curves recorded at different potential scanning rates from 30 to 110 mV s^{-1} in 1.0 M KOH solution (between -0.15 V *vs.* RHE and + 0.35 V *vs.* RHE) for the FeMn@BNPCFs-600 (a), FeMn@BNPCFs-700 (b), FeMn@BNPCFs-800 (c), FeMn@BNPCFs-900 (d) and FeMn@BNPCFs-1000 (e) samples.

Table S2 *C*, roughness (*R*), and electrochemical specific active area (ECSA) values for the catalysts modified electrodes and bare RDE. The *R* and ECSA values were calculated by using **Equations S1 and S2.**

Electrodes	***C*** **(mF cm^{-2})**	***R***	**ECSA (cm^2)**
Bare GCE	1.139	-	-
FeMn@BNPCFs-600	1.56	1.37	0.27
FeMn@BNPCFs-700	10.75	9.44	1.85
FeMn@BNPCFs-800	18.35	16.11	3.16
FeMn@BNPCFs-900	68.96	60.54	11.88
FeMn@BNPCFs-1000	16.68	14.64	2.87

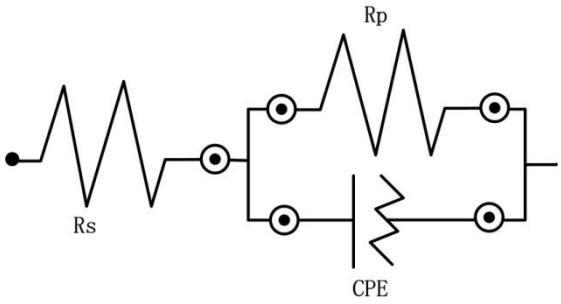

Figure S11. The equivalent electrical circuit utilized for fitting the electrochemical impedance spectra showed in **Figure 7e**.

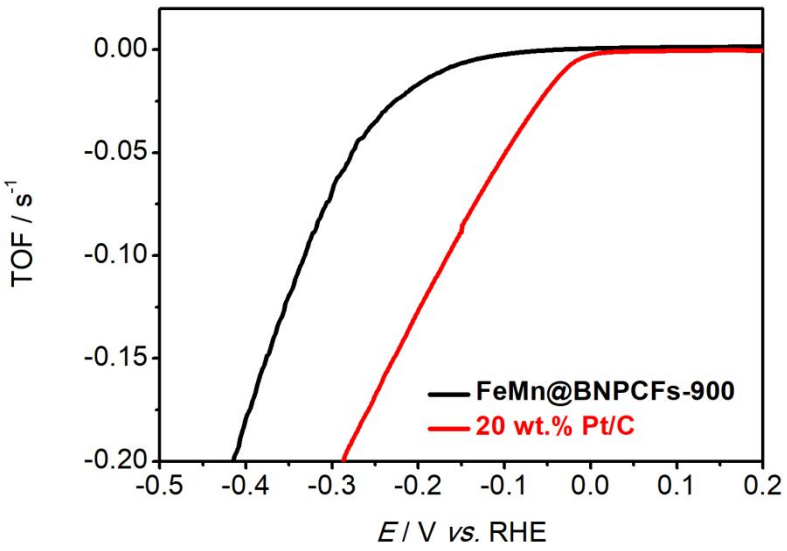

Figure S13.TOF values for the HER calculated at potentials between -0.5 and 0.20 V vs. RHE for 20 *wt.*% Pt/C and FeMn@BNPCFs-900 catalysts.

The turnover frequency (TOF) values of the optimal catalyst were calculated from the **Equation S3**. We first measured the Fe and Mn contents on the surfaces of FeMn@BNPCFs-900; for this, 1 mg of FeMn@BNPCFs-900 were first washed in the strong acid and further detected *via* the ICP technology. The ICP measurement results display that the mole numbers of Fe and Mn atoms on the surfaces of 1 mg FeMn@BNPCFs-900 sample are 6.875×10^{-4} mmol and 2.0618×10^{-3} mmol, respectively; demonstrating the most Fe_3C nanoparticles were imbedded into carbon layers. XPS test results have proved that the mole numbers of B and N elements in 1 mg of FeMn@BNPCFs-900 are 1.43×10^{-4} mmol and 3.0438×10^{-4} mmol, respectively. Assuming all Fe, Mn, B and N atoms dispersed along FeMn@BNPCFs-900's surfaces are catalytically active toward HER, the TOF values of the optimal

FeMn@BNPCFs-900 and 20 *wt.*% Pt/C catalysts were then calculated between -0.5 and 0.20 V *vs.* RHE in a 1.0 M KOH (as shown in **Figure S13**). The TOF values of FeMn@BNPCFs-900 calculated in the as-chosen potential range are all smaller than those of the 20 *wt.*% Pt/C catalyst.

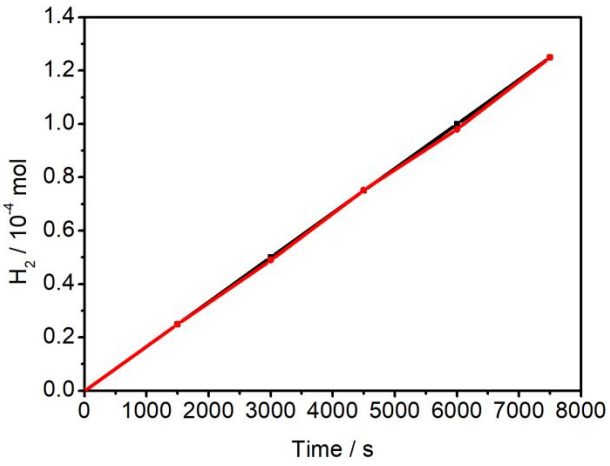

Figure S14. Amount of theoretically calculated (black) and experimentally measured (red) hydrogen versus time of FeMn@BNPCFs-900 under a static over-potential of 300 mV *vs.* RHE.

The generated gas was analyzed by gas chromatography (GC) analysis. The generated hydrogen was measured quantitatively using a calibrated pressure sensor to monitor the changes in pressure in the cathode compartment of an H-type electrolytic cell. Potentiostatic cathodic electrolysis was performed by maintaining a FeMn@BNPCFs-900 modified glassy carbon electrode at the over-potential of 300 mV for 7500 seconds. To calculate the Faradaic efficiency (FE) of the electrocatalytic hydrogen evolution process, we compared the amount of experimentally quantified hydrogen with the theoretically calculated hydrogen (assuming 100% FE). The agreement between both the theoretically and experimentally measured values suggests an FE of close to 100% (**Figure S14**).

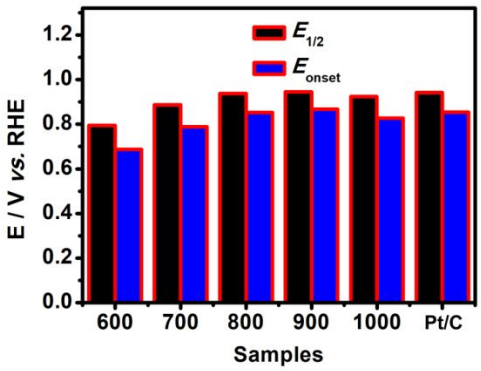

Figure S15. The corresponding ORR E_{onset} and $E_{1/2}$ values for the FeMn@BNPCFs-600, FeMn@BNPCFs-700, FeMn@BNPCFs-800, FeMn@BNPCFs-900, FeMn@BNPCFs-1000 and 20 *wt.*% Pt/C samples.

Table S3 A comparison on ORR catalytic data between our resultant catalysts and other reported non-precious metal based ORR catalysts.

Catalysts	E_{onset} (V vs. RHE)	$E_{1/2}$ (V vs. RHE)	j_L (mA cm^{-2})	Medium	References
FeMn@BNPCFs-600	0.795	0.688	-4.507	0.1 M KOH	This work
FeMn@BNPCFs-700	0.887	0.789	-4.924	0.1 M KOH	
FeMn@BNPCFs-800	0.938	0.853	-5.776	0.1 M KOH	
FeMn@BNPCFs-900	0.946	0.868	-5.976	0.1 M KOH	
FeMn@BNPCFs-1000	0.925	0.827	-5.310	0.1 M KOH	
20 wt.% Pt/C	0.943	0.854	-5.449	0.1 M KOH	
Fe@Mn13-polymer	0.78	0.7	-2.5	0.1 M KOH	*Dalton Trans.* **2019**, *48*,4794-4797
Fe,Mn,N-FGC	1.03	0.89	-6.47	0.1 M KOH	*Inorg. Chem.* **2020**, *59*, 5194–5205
Fe,Mn-N/C-900	0.934	-	-6.1	0.1 M KOH	*J. Mater. Chem. A* **2018**, *6*, 13254-13262
Fe/Mn-N-C	-	0.9	-6.05	0.1 M KOH	*Nature Commun.* **2015**, *6*, 8618–8626
FeNC-1000	-	0.9	-5.8	0.1 M KOH	*ACS. Appl. Mater. Interfaces* **2018**, *10*, 10778-10785
Mn@NPC-NH_3	0.95	0.83	-5.69	0.1 M KOH	*ACS. Sustainable. Chem. Eng.* **2020**, *8*, 12618-12625
Mn-Fe-N/S@mC	0.93	0.89	-6	0.1 M KOH	*Nano Energy* **2019**, *63*, 103851
Mn/C-NO	0.92	0.86	-5.6	0.1 M KOH	*Adv. Mater.* **2018**, *30*, 1801732
Mn-N-C	0.98	0.86	-5.8	0.1 M KOH	*Int. J. Hydrogen Energ.* **2019**, *44*, 26387-26395.
BN-CDs@CNT	0.92	0.8	-5.9	0.1 M KOH	*J. Colloid Interface Sci.* **2021**, *600*, 865-871
CNx/CBx-GNRs	0.8	-	-3.75	0.1 M KOH	*ACS Appl. Mater, Interfaces* **2015**, *7*, 7786-7794
Mn_2Co_3-900	0.91	0.76	-5.8	0.1 M KOH	*J. Mater. Chem. A* **2019**, *7*, 20649-20657.
Fe_3Mn_1/NCNTs-100	0.91	0.86	-5.4	0.1 M KOH	*ChemCatChem* **2018**, *10*, 5475-5486.

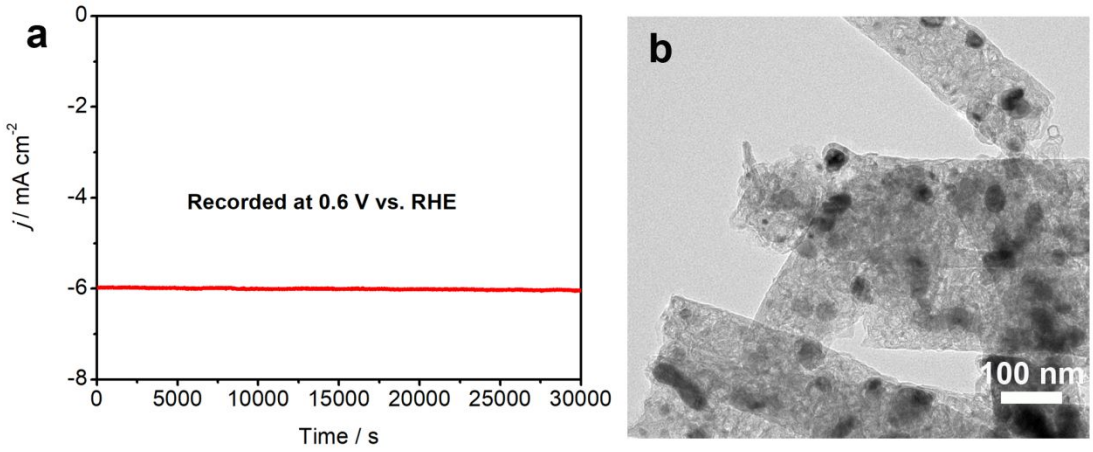

Figure S16. **(a)** Time dependence of the current density for FeMn@BNPCFs-900 at a static potential of 0.6 V vs. RHE for 30000 s in O_2-saturated 0.1 M KOH. **(b)** TEM image of the FeMn@BNPCFs-900 sample after the accelerated durability test in O_2-saturated 0.1 M KOH solution.

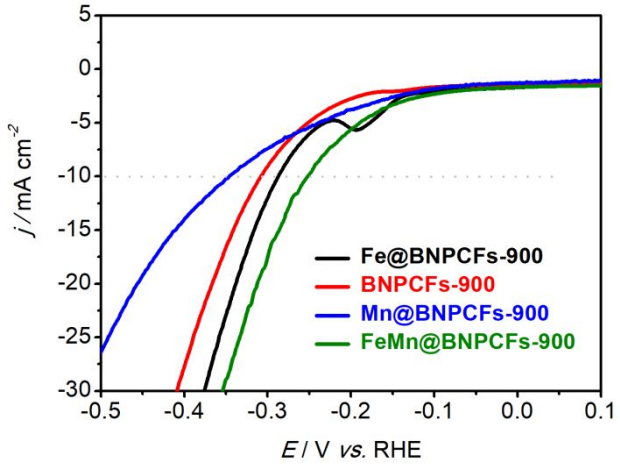

Figure S17. The HER LSV polarization curves recorded in 1.0 M KOH for FeMn@BNPCFs-900, Fe@BNPCFs-900, Mn@BNPCFs-900 and BNPCFs-900 control samples.

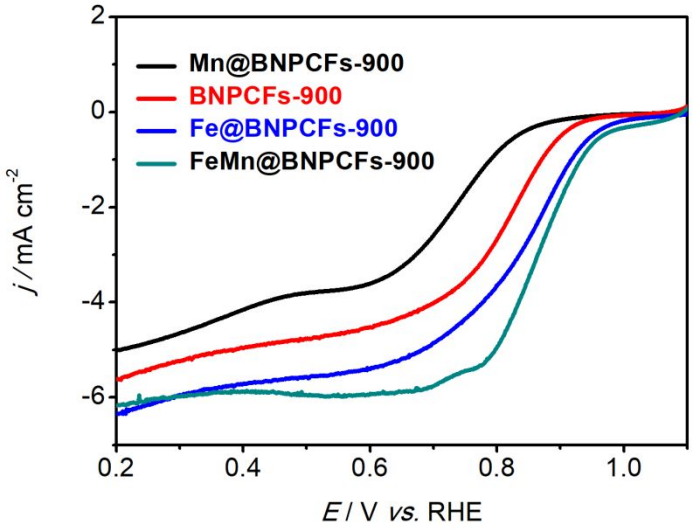

Figure S18. The ORR LSV polarization curves recorded in 0.1 M KOH for FeMn@BNPCFs-900, Fe@BNPCFs-900, Mn@BNPCFs-900 and BNPCFs-900 control samples.